

# Correction of the phase retardation caused by intrinsic birefringence in deep UV lithography

Alexander Serebriakov\*, Florian Bociort, Joseph Braat

Optics Research Group, Delft Univ. of Technology, Lorentzweg 1, 2628 CJ Delft, The Netherlands

## ABSTRACT

In the year 2001 it was reported that the birefringence induced by spatial dispersion (BISD), sometimes also called intrinsic birefringence, had been measured and calculated for fluorides  $\text{CaF}_2$  and  $\text{BaF}_2$  in the deep UV range. It was also shown that the magnitude of the BISD in these cubic crystals is sufficiently large to cause serious problems when using  $\text{CaF}_2$  for lithographic objectives at 157 nm and possibly also in the case of high numerical aperture immersion objectives at 193 nm. Nevertheless the single-crystal fluorides such as  $\text{CaF}_2$  are the only materials found with sufficient transmissivity at 157 nm and they are widely used at 193 nm for chromatic correction. The BISD-caused effects lead to the loss of the image contrast. In this work we discuss issues related to the design of optical systems considering the BISD effect. We focus on several approaches to the compensation of the BISD-related phase retardation and give examples of lithographic objectives with the compensated phase retardation.

Keywords: lithography, birefringence, spatial dispersion, phase retardation, optical system design

## 1. INTRODUCTION

The presence of the BISD effect in crystals at short wavelengths was a surprise for the lithography industry that has caused considerable difficulties for 157 nm lithography [1]. Lithography equipment manufacturers were already familiar with stress-induced birefringence in calcium fluoride and they were prepared to compensate it with relatively complex lens designs. However intrinsic birefringence is able to inflict several times more birefringence than allowed, creating fuzzy images at the wafer. A number of theoretical studies of the BISD in the cubic crystals were completed and the detailed description for the effect can be found in [2]-[8]. Results of this intensive research were implemented in optical design software [9]. Some issues in the optical system design were discussed in [8]. It was shown, for instance, that the standard deviation of the retardation over the pupil is a good indicator for the BISD influence on the image quality.

In optical system design, BISD leads to the appearance of multiple polarized rays during refraction. There are two basic effects depending on crystal orientation, wavelength, thickness and shape of the lens. The first BISD consequence is the appearance of an optical path-length difference between the two orthogonally polarized components corresponding to a ray. This path-length difference, resulting in a phase retardation, can be visualized in pupil maps for arbitrary field points (Fig. 1 a). It is not only the magnitude of the phase retardation which is important for an analysis of the total phase retardation but its orientation as well. After refraction into a lens, this orientation can be defined as the orientation of the projection of the fast eigenvector onto the pupil plane (Fig. 1 b). The phase retardation caused by BISD leads to a loss of image contrast.

The second consequence of BISD is a small angular difference in ray paths. In an optical system with  $N$  components, for each incident ray on the first surface there are  $2^N$  outgoing rays at the image plane. Such multiple ray sets produce transmitted wave fronts, which may or may not substantially overlap in the exit pupil and in the image plane. The bifurcation of the rays leads to an angular difference in ray path between ordinary and extraordinary rays after each refraction, which results in a ray deviation at the image plane. This effect requires special consideration and will be considered in a subsequent paper.

---

\* [a.serebriakov@tnw.tudelft.nl](mailto:a.serebriakov@tnw.tudelft.nl); (+31) 15 2788109; <http://www.optica.tn.tudelft.nl>

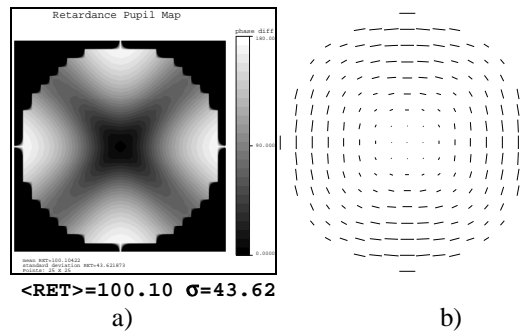


Fig. 1. Visualization of the phase retardation: a) pupil map of retardation magnitude; it changes within the range of  $0 \dots 180^\circ$ . The dark tone indicates regions with low phase retardation and light tone indicates ones with high phase retardation.  $\langle \text{RET} \rangle$  is the average retardation value and  $\sigma$  is the standard deviation over the pupil; b) pupil map of retardation orientation where orientation of each line indicates the fast-axis orientation.

The basic idea of the phase compensation is the following. It is not possible to avoid the spatial birefringence effect completely (that would require zero angles between rays and an optical axis of the crystal), but it is possible to achieve a certain distribution of the retardation magnitude and retardation orientation in the pupil plane. Since the contribution of components (or group of components) to the total phase retardation are additive, it is possible to combine two predefined distributions of the phase retardation with the same magnitude but orthogonal orientation. By summation these two distributions can cancel each other (Fig. 2). The different methods proposed for obtaining desired phase distribution are discussed in this paper.

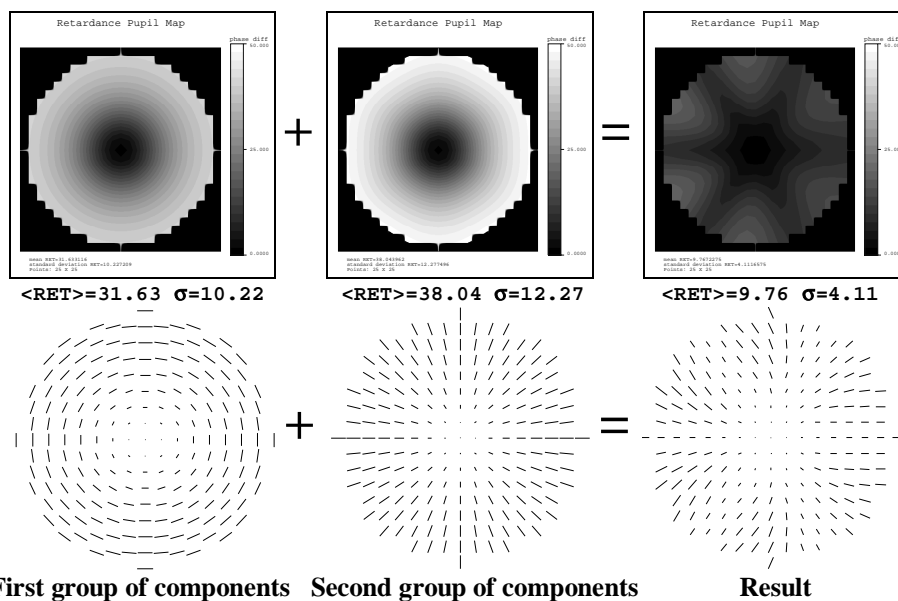


Fig. 2. Basic compensation of the phase retardation. Two components with the same distribution of the retardation magnitude but orthogonal retardation orientation give much smaller resulting retardation magnitude.

According to our experience the effect can be considered as compensated if the value of the standard deviation of the residual phase retardation does not exceed  $10\text{--}20^\circ$ , depending on specifications of the objective. In this case the contrast loss caused by the BISD-effect is smaller than the image deterioration caused by aberrations and other unavoidable polarization effects induced by high-NA, coating, residual stress-induced effects i.e. There is not too much difference between phase compensation for 193 and 157 nm objectives, because the character of the effect remains the same and only the magnitude of the linear birefringence scales up with lowering the wavelength.

## 2. COMPENSATION OF PHASE RETARDATION

### 2.1. Crystal Axis Clocking

One of the major obstacles for the BISD compensation is the possible effect of asymmetry of the pupil map around the center of the pupil. For preserving the symmetry only three types of directions in the cubic crystal namely  $\langle 001 \rangle$ ,  $\langle 110 \rangle$  and  $\langle 111 \rangle$  can be selected as an optical axis. The pupil maps for these crystal orientations are discussed in Ref. [8]. They are also shown on the right side of Fig. 4-6. In order to define some intermediate positions it is convenient to introduce the notation where in addition to crystal orientations we define the orientation of the pupil map (angle  $\psi$  counted in a clockwise direction) as  $\langle \text{crystal orientation} \rangle - \psi$  e.g.  $\langle 001 \rangle - 0^\circ$ ,  $\langle 100 \rangle - 45^\circ$ ,  $\langle 111 \rangle - 0^\circ$ ,  $\langle 111 \rangle - 60^\circ$  etc (Fig. 4-6).

We will show that it is very useful for our investigation to determine the contribution of separate components in the cumulative phase retardation of an objective for lithography. For this purpose, we classify optical components according to their contribution to the cumulative phase retardation. The phase retardation for each component was computed and normalized to the maximum value for each case. In order to define the maximal possible contribution, the computations were made with a marginal ray for the crystal orientations  $\langle 001 \rangle$  and  $\langle 111 \rangle$ . Because the phase retardation distribution is monotonic, only one ray needs to be traced for these directions. For the  $\langle 011 \rangle$  direction, however, the difference between center and edge of the pupil must be computed, because both have non-zero retardation value. In this case at least two rays, the marginal one and the ray along the optical axis, have to be traced. It should be pointed out that for the  $\langle 011 \rangle$  direction the distribution can be inverted when the retardation at the edge is higher than the retardation in the center of the pupil. This happens, for instance, in biconcave lenses, when the edge thickness is much larger than the center thickness.

An optical system with components gray-scaled according to their phase retardation contribution is shown in Fig. 3. (The specifications of this system were taken from Ref. [10].) It can be seen that for the  $\langle 001 \rangle$  and  $\langle 111 \rangle$  orientations only a few components contribute significantly to the cumulative retardation. For the  $\langle 011 \rangle$  direction, several components have a significant contribution. This phase retardation contribution mostly depends on the lens thickness and more lenses have significant contribution.

The regular nature of the BISD intuitively leads to the "clocking" solution, which is widely used today in 248 and 193-nm lithography in order to adjust for aberrations caused by deviations of the lens surfaces [11]-[14]. Clocking adjusts the lens elements by rotation in a plane perpendicular to the system axis. However, using clocking for the compensation of phase retardation limits the possibility of using clocking later on to adjust for the unavoidable defects of the lens elements. The references mentioned above discuss the compensation approach for certain types of optical systems. We will summarize all approaches and describe the general strategy of the compensation of phase retardation in what follows.

The first step is the creation of a circular distribution of the phase retardation over the pupil. As it can be observed from Fig. 4-6, different crystal orientations along the system axis have different angular symmetry of the retardation distribution. It is thus possible to tune the separate components to achieve the desired distribution of the retardation over the pupil by adjusting of the phase retardation contributions of several components. So, by combining lenses with orientations  $\langle 001 \rangle - 0^\circ$  and  $\langle 001 \rangle - 45^\circ$  for the  $\langle 001 \rangle$  direction or  $\langle 111 \rangle - 0^\circ$  and  $\langle 111 \rangle - 60^\circ$  for the  $\langle 111 \rangle$  direction, we can achieve almost circular distributions of the phase retardation magnitude (see Fig. 4-5). It is seen that regions in the pupil with low phase retardation overlap with those having a high phase retardation value. These two rotated components (or groups of components) with overlapping pupil maps should give the same contribution. It is seen from the figures that, as a result of the combination of  $\langle 001 \rangle - 0^\circ$  and  $\langle 001 \rangle - 45^\circ$ , we have tangential orientation of the phase retardation for any pupil point, and for the couple  $\langle 111 \rangle - 0^\circ$  and  $\langle 111 \rangle - 60^\circ$  we have radial orientation of this value. It should be pointed out that for two plates  $\langle 111 \rangle$  and  $\langle 001 \rangle$  with equal thicknesses the magnitude of the phase retardation for the  $\langle 111 \rangle$  direction is lower, i.e. the path length in glass for this components should be larger in order to obtain the same contribution as for the  $\langle 001 \rangle$  direction.

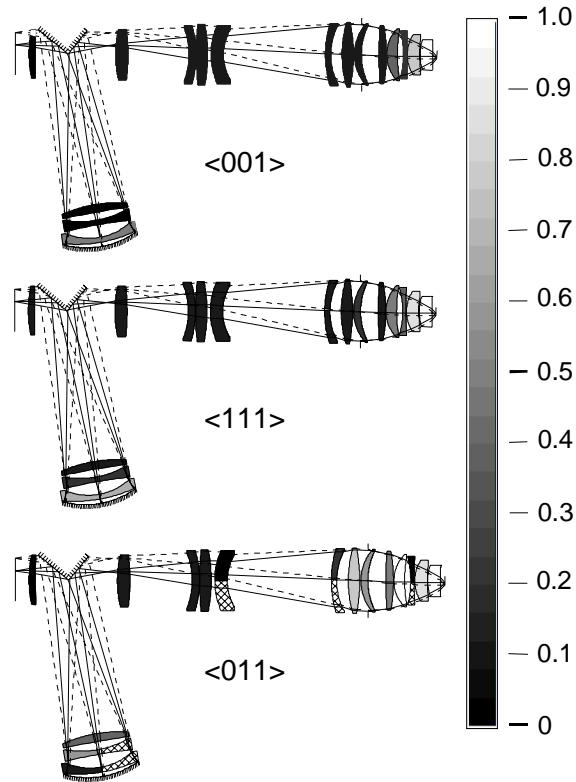


Figure 3. Contribution of separate components to the cumulative phase retardation depending on the chosen crystal orientation (all components are oriented along the crystal orientation shown below). A light tone indicates components with high contribution. For the  $\langle 011 \rangle$  direction, the elements with inverted retardation value distribution (with highest retardation value at the edge) are partially hatched.

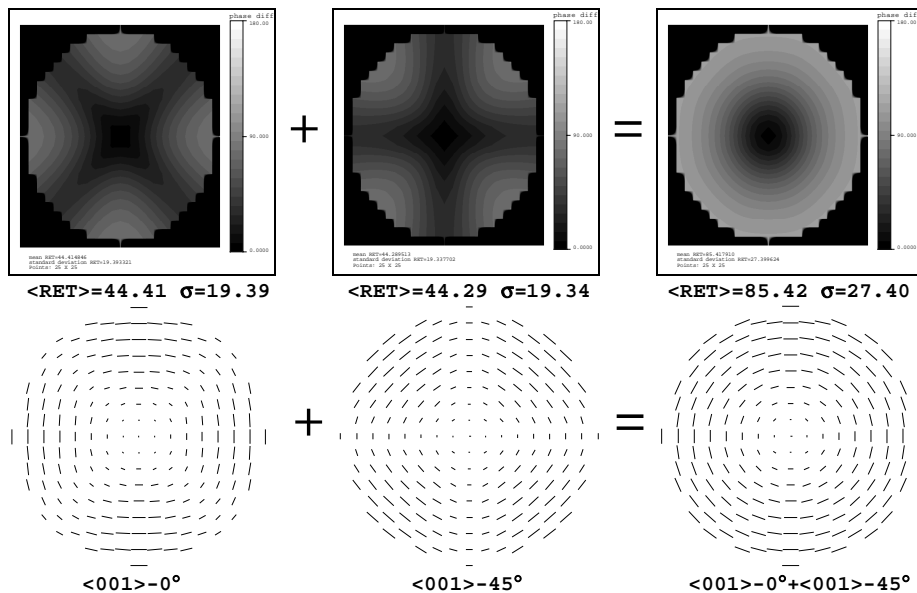


Fig. 4. Obtaining a circular distribution of the phase retardation for the  $\langle 001 \rangle$  direction. The resulting magnitude of the phase retardation has a circular distribution and tangential orientation.

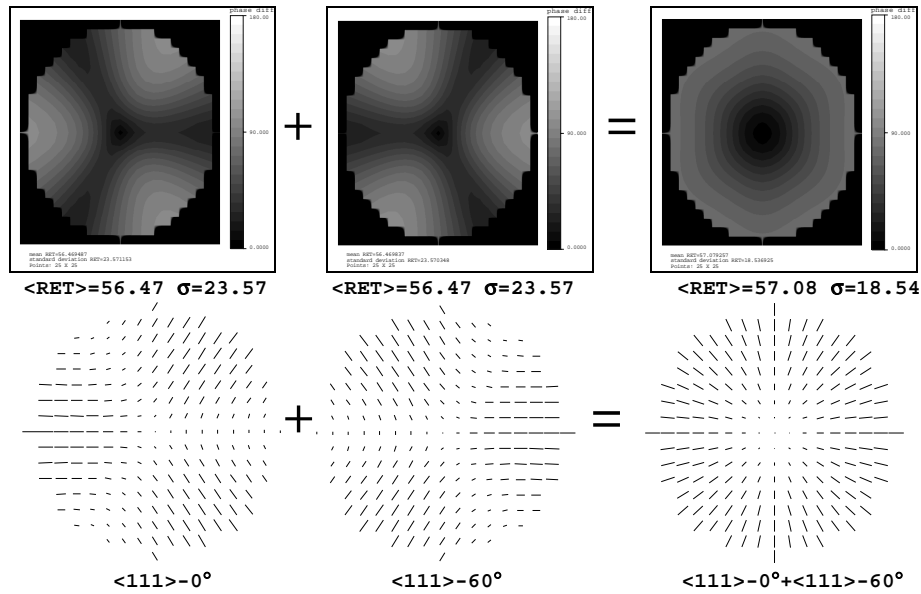


Fig. 5. Obtaining a circular distribution of the phase retardation for the  $\langle 111 \rangle$  direction. The resulting magnitude of the phase retardation has a circular distribution and the radial orientation.

It is also possible to obtain a circular distribution for the  $\langle 011 \rangle$  direction (Fig. 6). However, in this case at least four components should be used for obtaining a circular phase retardation. In principle, the shown pupil maps allow to combine them in any way in order to obtain desired phase retardation distributions.

The second step is the nulling of the phase retardation. By inspecting the phase retardation pupil maps shown in Fig. 4-6 it can be seen that the resulting orientation of the retardation for the  $\langle 001 \rangle$  clocked pair is orthogonal to the orientation for the  $\langle 111 \rangle$  clocked pair (or the orientation for the  $\langle 011 \rangle$  clocked quartet). That means that the retardation has opposite sign for these combinations. Thus when the magnitude of the retardation is also equal then combining these lens blocks consisting of two or four lenses can be used to reduce or null out the total retardation value. The results of this compensation can be seen in Fig. 7.

## 2.2. Crystal clocking applied to a practical system

We will now apply the crystal axis clocking approach to the optical system shown in Fig. 3. In the first stage, we compute the phase retardation contribution of components for the three basic crystal orientations and then we classify the components according their values (see Table 1 and corresponding grayscale maps in Fig. 3). In this case we use a combination of  $\langle 111 \rangle$  and  $\langle 001 \rangle$  directions.

In the next step, for forming a circular distribution, we choose the crystal orientation of certain components as discussed below. As it is seen from Table 2 we were able to achieve equal cumulative retardation value for two directions in each of the two couples of the  $\langle 111 \rangle$  and  $\langle 001 \rangle$  directions. The ratio between the cumulative retardation values for the  $\langle 111 \rangle$  and  $\langle 001 \rangle$  directions is chosen to null the total retardation. Finally, the components are oriented along the direction shown in the last column of Table 1. We note that in this example some components, close to the spherical mirror, are used double pass and should have the same crystal orientation in both directions. Moreover for the  $\langle 111 \rangle$  direction, the components which have pupil maps rotated over  $180^\circ$ , because of opposite angle between marginal ray and optical axis, are shown as well (between brackets we show the orientation entered into the software).

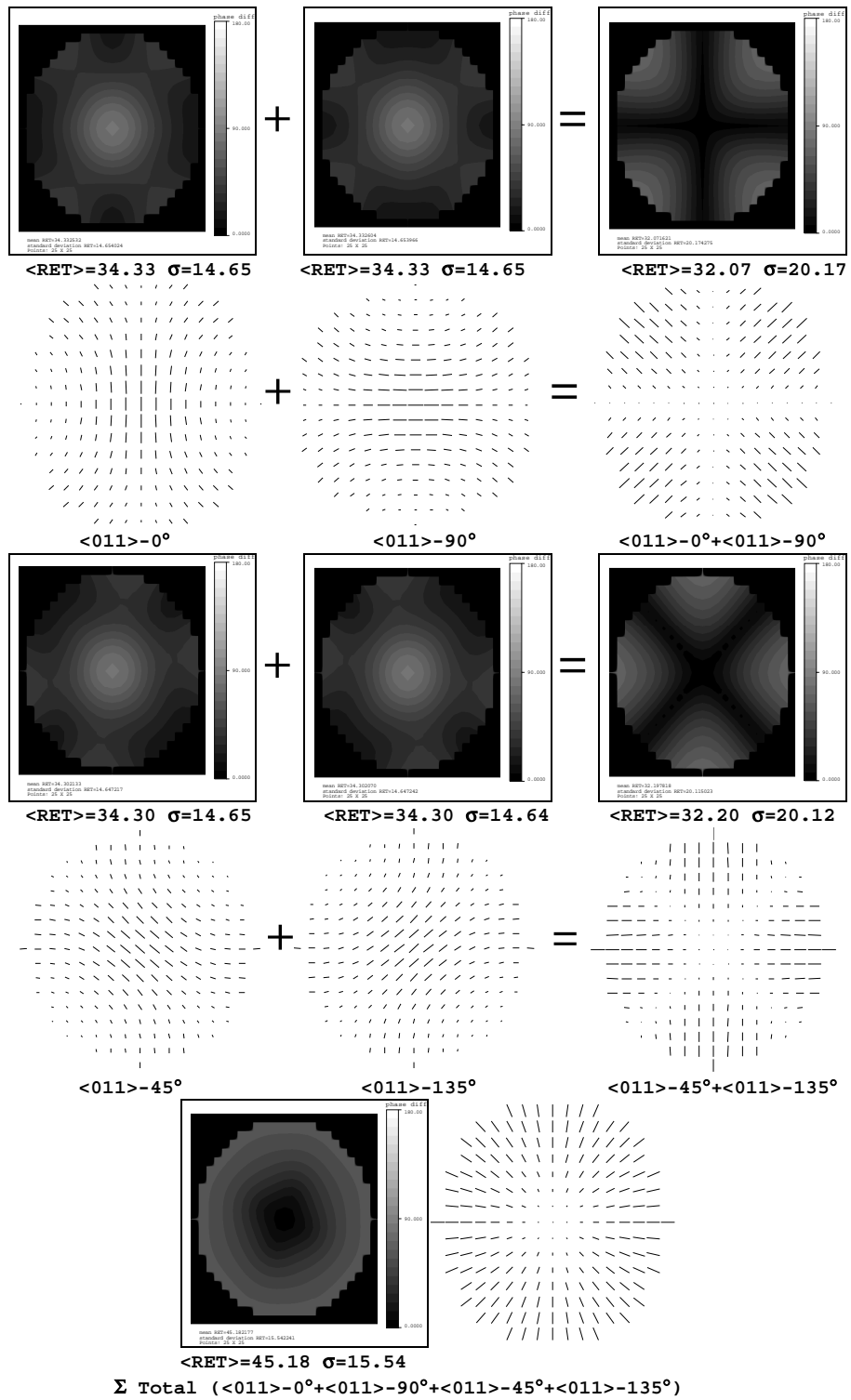


Fig. 6. Obtaining a circular distribution of the phase retardation for  $\langle 011 \rangle$  direction. The resulting magnitude of the phase retardation has a circular distribution and radial orientation. This approach requires four components. The intermediate cumulative pupil maps have cross-like retardation distributions.

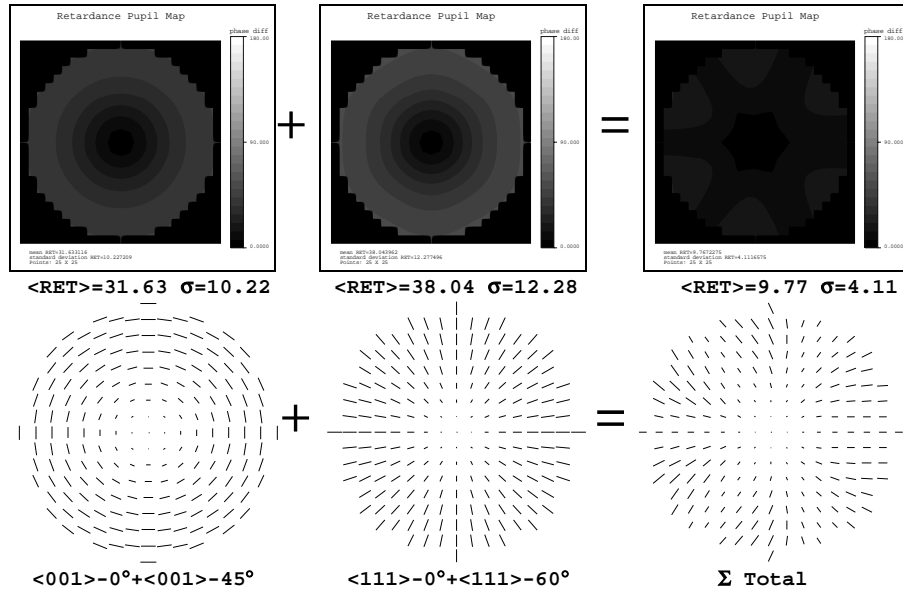


Fig. 7. Nulling the phase retardation by crystal axis "clocking". Two sets of components with the same distribution of the phase retardation but having opposite orientation result in a very small total retardation value.

Table 1. Phase retardation contribution of the separate components in the example system.

Component #	Surface #	Phase retardation contribution for <001> direction	Phase retardation contribution for <111> direction	Crystal orientation of the component
1	46	59.32751	89.97305	111-0°
2	44	40.50317	68.84210	001-0°
3	12	24.87031	50.15022	111-60°
4	9	24.21614	49.53407	111-60°(as #12)
5	40	20.76436	37.54656	001-45°
6	42	8.123430	23.39501	001-45°
7	35	4.667793	15.98327	001-45°
8	14	3.341908	20.71335	001-45°
9	7	2.976251	19.91663	001-45°(as #14)
10	25	2.056147	15.77146	001-0°
11	5	1.338430	1.991897	001-45°
12	31	1.325586	2.469966	001-45°
13	16	1.313316	2.550029	001-45°(as #5)
14	29	1.286954	3.685012	111-60°
15	23	1.121591	16.89479	111-0°(111-60°)
16	33	0.813918	6.257399	111-0°(111-60°)
17	38	0.544681	10.22191	001-0°
18	27	0.474838	13.69446	001-0°
19	2	0.086460	9.325174	111-60°(111-0°)

Table 2. Combining components with different crystal orientation for forming a circular distribution of the phase retardation and its compensation.

Orientation	001-0°	001-45°	111-0°	111-60°
Contribution of Components	2.056147	1.33843	16.89479	9.325174
	0.474838	2.976251	6.257399	49.53407
	0.544681	3.341908	89.97305	50.15022
	40.50317	1.313316		3.685012
		1.325586		
		4.667793		
		20.76436		
	8.12343			
$\Sigma$	43.57883	43.85107	113.1252	112.6945

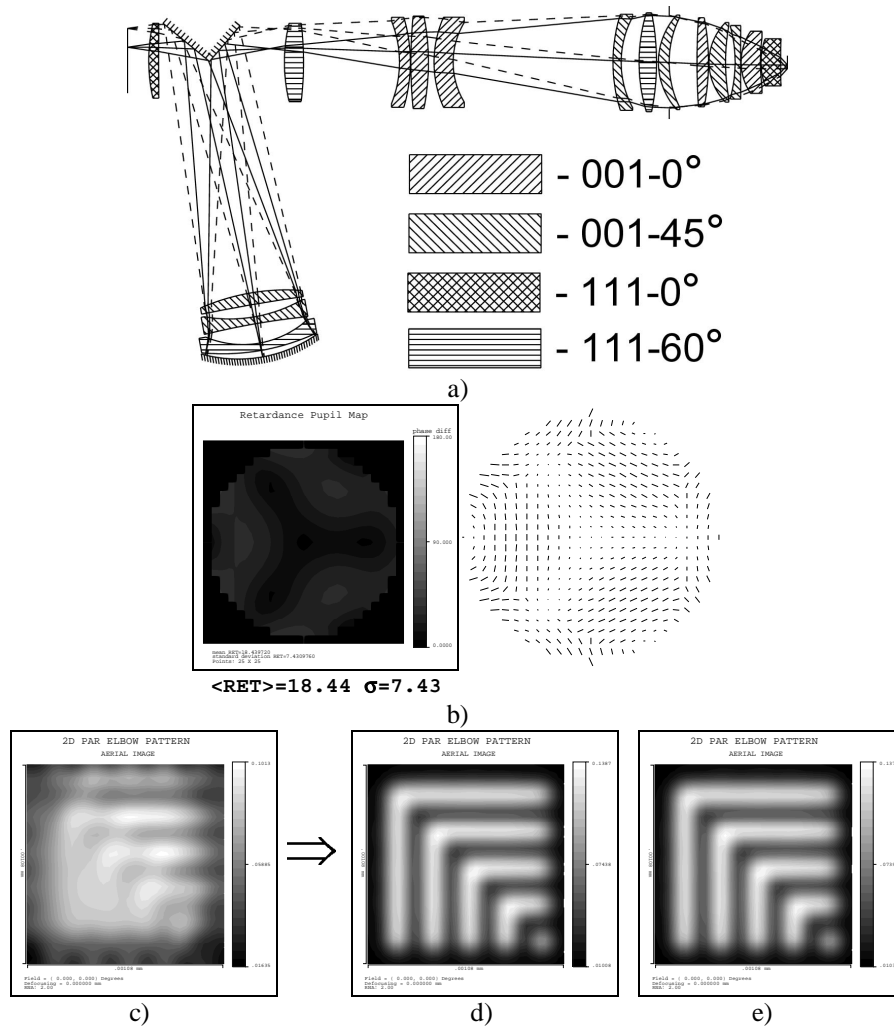


Fig. 7. Results of the phase retardation compensation: a) optical system with compensated phase retardation (the crystal orientation of the components is shown); b) pupil map for the compensated system; c) simulated image of the test-object for the uncompensated system; d) simulated image of the test-object for the compensated system; e) simulated image of the test-object for system without including the BISD-effect. (Ray bifurcation is not included in the simulation in all cases.)



The result of this compensation is shown in Fig. 7. The presented pupil map shows that the phase retardation is very well balanced and the image of the 2D test-object is drastically improved. For comparison, we also show the image of the 2D test-object for the same objective in the absence of the BISD-effect. If a further improvement is required then it is possible to adjust the thickness of components. In this case the merit function for thickness optimization should be extended by adding the value of the standard deviation of retardation.

The BISD compensation for off-axis points is more difficult, because the distribution of the birefringence is not symmetric, but in general the behavior for such a field point is comparable to that of the axial point. In all cases studied by us the compensation for the axial point helps the compensation for the off-axis points.

Generally speaking each type of lithographic objective requires a specific compensation approach. For instance, the optical system shown in Fig. 8 [15] consists of eight optical components and it has a relatively small total track in glass. This makes this system very attractive because of small ray deviation caused by BISD. However, the approach discussed above cannot be applied because the phase retardation given by different components have different order of magnitude. The small number of components is not sufficient for the use four basic crystal orientations ( $\langle 001 \rangle$ - $0^\circ$ ,  $\langle 001 \rangle$ - $45^\circ$ ,  $\langle 111 \rangle$ - $0^\circ$ ,  $\langle 111 \rangle$ - $60^\circ$ ) which should have the same order of magnitude of the phase retardation in order to correct it.

For the compensation of phase retardation in this optical system another approach was applied. It turns out that for this system the contributions of separate components are of the same order of magnitude if they are oriented along  $\langle 011 \rangle$  directions. Moreover most components are situated in the part of the system where the marginal ray angle with the optical axis is not large and the pupil maps of certain components possess only the central zone of the typical pupil maps for the  $\langle 011 \rangle$  directions shown in Fig. 6. It is seen from this figure that in the region, close to the optical axis, the orientations of the phase retardation for crystal orientations  $\langle 011 \rangle$ - $0^\circ$  and  $\langle 011 \rangle$ - $90^\circ$ , are orthogonal. Thus we can use only one clocked crystal orientation in order to compensate the phase retardation. The selection of the orientation of the components in the optical system was done on the basis of the method described above, with classification by the single component contribution in the cumulative phase retardation. The orientation of the components, cumulative pupil maps for  $\langle 011 \rangle$ - $0^\circ$  and  $\langle 011 \rangle$ - $90^\circ$  and the final compensation result are shown in Fig. 8 b).

As in the case of the first example, such an arrangement allows to compensate the effect without or with minor additional optimization and does not break the geometrical aberration correction. In all cases the final compensation can be done by adjustment of the lens thicknesses.

On the basis of our experience we propose a general strategy with the following steps:

- Computation of the pupil maps for basic crystal orientations ( $\langle 001 \rangle$ ,  $\langle 111 \rangle$ ,  $\langle 011 \rangle$ ) for each component assuming that this component is the only one with the phase retardation.
- Classification of components according to their contribution to the cumulative phase retardation.
- Select a compensation strategy depending on number and position of components, thicknesses, balance contributions, total track in glass etc.
- Apply this compensation strategy to the optical system.
- Final optimization including rotation of crystals, adjustment of lens thickness and curvatures.

### 2.3. Correction of the phase retardation with the aid of stress-induced birefringence

Another compensation approach describes the use of a photoelastic effect for the BISD compensation [16]. The stresses applied for obtaining stress-induced birefringence can be caused by tension, pressure, changing thermal gradients in crystals or by ion diffusion.

This effect can also be modeled and analyzed with the help of modern optical software such as Code V [9],[16]. In Fig. 9 we show the example of compensation of the phase retardation for the optical system shown in Fig. 8. In this case we apply stress to the component situated near the system stop because in this case the contributions for all field positions are similar. As seen from the drawings, the effect can be very well compensated. However, in practice it is very difficult to correct the large retardation value without risk of destroying the components. It is also unclear how to change the orientation of the phase retardation when tensions or stresses should alternate within one component. The sharp separation between orientation of the phase retardation in the neighboring pupil positions should be avoided as well. In our view this method can be successfully applied for the compensation of the residual phase retardation remaining after clocking.

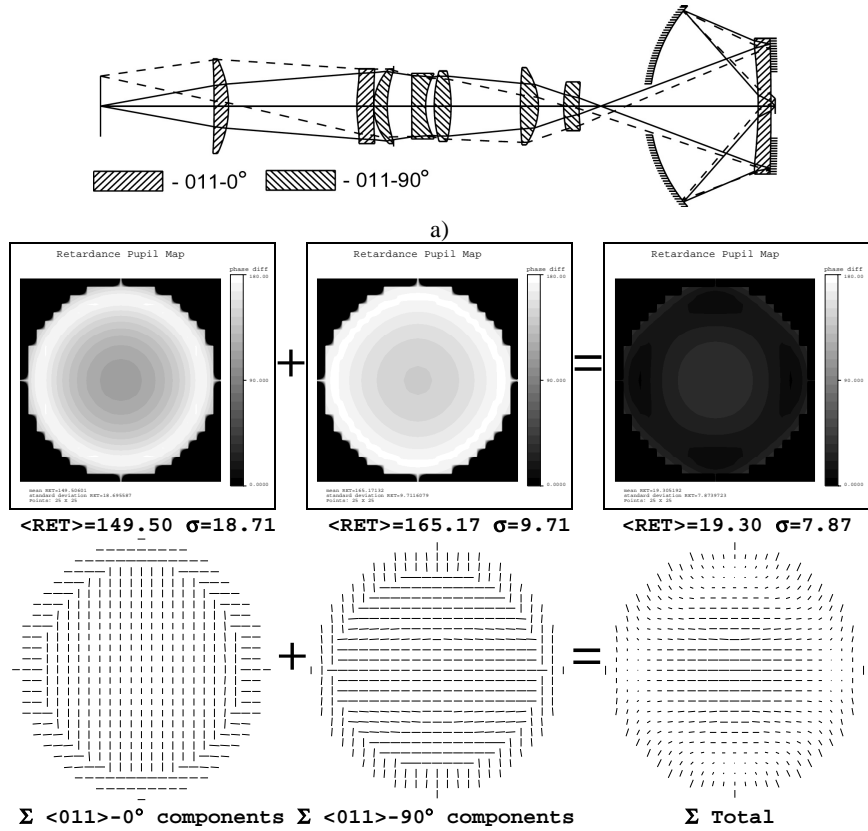


Fig. 8 Compensation of the phase retardation in a DUV lithographic system with small number of components. a) optical system layout; b) phase retardation pupil maps of cumulative retardation for  $\langle 011 \rangle - 0^\circ$  and  $\langle 011 \rangle - 90^\circ$  directions and total retardation value.

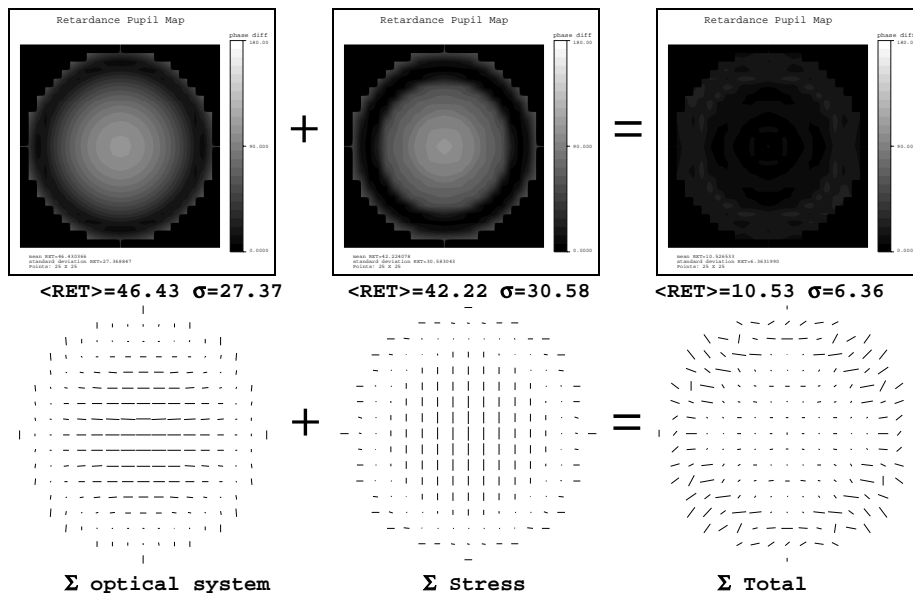


Fig. 9. Compensation of the phase retardation by stress-induced birefringence. In the left picture the total phase retardation of the system without applied stress is shown. In the middle we see the phase retardation pupil map of the compensator. In the right hand picture, the total phase retardation distribution is presented.

## 2.4. Correction of the phase retardation with birefringence compensator

Some references suggest the use of the natural crystal anisotropy for the correction of spatial dispersion [18]. There are media, transparent in the deep UV range, which have a too large birefringence value to be used as lenses, but thin compensator plates produced from such a material can contribute a small birefringence value. Examples of these materials with natural birefringence are uniaxial crystals such as SiO<sub>2</sub>, Al<sub>2</sub>O<sub>3</sub>, MgF<sub>2</sub>, LaF<sub>3</sub>.

### 2.4.1. One-plate retardation compensator

A simple phase retardation compensator can be produced with one plate. For the radially symmetric distribution of the phase retardation the optical axis of the crystal should be oriented along the system axis. The example of this one-plate compensator for the point object on the optical axis is shown in Figure 10.

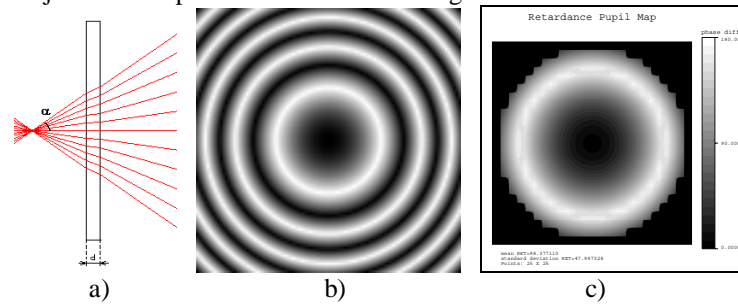


Fig. 10. One plate retardation compensator: a) one-plate compensator, b) theoretically computed retardation pupil map; c) pupil map obtained with optical design software.

The circular distribution of the phase retardation distribution suggests to use it for the compensation of the circular distribution of the phase retardation obtained with  $\langle 001 \rangle$ -0° and  $\langle 001 \rangle$ -45° or  $\langle 111 \rangle$ -0° and  $\langle 111 \rangle$ -60° combinations (Fig. 3 and 4). In this case the first "retardation ring" in the distribution shown in Fig. 10 b) can be superimposed with the ring obtained by clocking. The position for the compensator in the optical system can be chosen near the object point (for adjustment of the retardation value for different field points) or near the system stop. This solution has, however, a disadvantage because large phase retardation values cannot be obtained without a strong increase of the ray deviation caused by bifurcation.

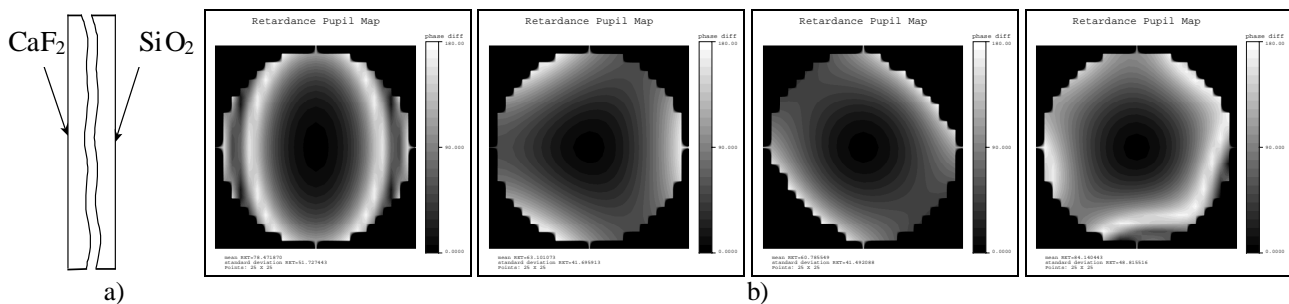


Fig. 11. a) Two-component compensator. b) Phase retardation pupil maps obtained with different inner profiles of the two-plate compensator. The shape of the surface was modeled with the aid of Zernike polynomials.

### 2.4.2. Two-component compensator

In this compensation approach we use two plates. One of them is made from a cubic crystal material and the other from a crystal with natural birefringence, transparent in the deep UV (SiO<sub>2</sub>, Al<sub>2</sub>O<sub>3</sub>, MgF<sub>2</sub>, LaF<sub>3</sub>). The indices of refraction should be as close as possible. The outer surfaces of these plates are plane and the inner surfaces are identical and separated by a thin air space. Therefore this thin-plate construction does not actually influence the ray path but has a great impact on the state of polarization and consequently on the phase retardation of the rays. The inner surface profile can be optimized in order to minimize the total phase retardation of the objective. This plate construction can be positioned e.g. in the stop of the optical system. By changing the shape of the inner profile it is possible to obtain various retardation pupil maps (Fig. 11). More complex distributions or combinations of the shown maps are possible.

In principle, this approach offers the widest possibilities for compensation because the shape of the surface can be tuned in order to adjust it to the phase retardation distribution to be compensated. However, large values of the phase retardation cannot be compensated for the same reason we found with the one-plate compensator: the ray deviation value becomes unacceptably large. Thus this approach cannot be used on its own but can be used in combination with clocking for the compensation of residual stresses and residual BIRD values.

## CONCLUSIONS

We have discussed three approaches for the compensation of the phase retardation. All approaches assume the presence in the optical system of two groups of components contributing with almost the same distribution of the retardation magnitude but with the orthogonal retardation orientation. The first concept (clocking) uses the different dependence of the phase retardation for different crystal orientations. It was shown that by combining them in a certain way it is possible to reduce the image quality loss significantly. Several approaches for this combination of the crystal orientation were discussed. It is also possible to use the photoelasticity effect for the phase retardation compensation. In this case it is possible to introduce stress or tension in the crystal body to achieve the desired distribution of the retardation. This approach can be quite successful but has "mechanical" limits. The last approach exploits natural crystal birefringence for compensation. The results of the compensation are also promising; for instance, the retardation distribution can be asymmetrical with respect to the center of the pupil, which is difficult to realize with the clocking strategy. However, for a large value of the phase retardation the ray deviation introduced by the compensator exceeds the resolution limit. The main conclusion of this paper is that the phase retardation effect in deep UV lithography can be compensated. Explicit methods of compensation are presented. This compensation requires an additional effort from the optical designer and limits certain other possibilities in the optical design; but in our view the phase retardation effect on image quality can be reduced to a sufficiently low level.

## ACKNOWLEDGMENT

The first author gratefully acknowledges the support of this research by ASM Lithography.

## REFERENCES

1. John H. Burnett, Zachary H. Levine, and Eric L. Shirley "Intrinsic birefringence in calcium fluoride and barium fluoride", *Phys. Review B*, **64**, p. 241102 (2001);
2. H.A. Lorentz, *Collected papers*, Vol. 2-3 (Nijhoff, Den Haag, 1936);
3. V. M. Agranovich, V. L. Ginzburg, *Crystal Optics with Spatial Dispersion, and Excitons* (Nauka, Moscow, 1979)
4. John H. Burnett, Zachary H. Levine, Eric L. Shirley, and John H. Bruning, "Symmetry of spatial-dispersion-induced birefringence and its implications for CaF<sub>2</sub> ultraviolet optics", *JM<sup>3</sup>*, **1**, p. 213-224 (2002);
5. A. Rosenbluth, G. Gallatin, N. Seong, O. Dittmann, and M. Totzeck, "Image Formation In A Lens With Spatial Dispersion (Intrinsic Birefringence)" presented at 4th Int. Symp. on 157 nm Lithography, Yokohama, Japan (2003).
6. A. G. Serebryakov, F. Bociort, and J.J.M. Braat, "Spatial dispersion of crystals as a critical problem for deep UV lithography", *Journal of Optical Technology*, **70**(8), p. 566-569 (2003).
7. A. Serebriakov, E. Maksimov, F. Bociort, and J.J.M. Braat, "The effect of intrinsic birefringence in deep UV lithography", *Proc. SPIE 5249*, p. 624-635 (2004)
8. A. Serebriakov, E. Maksimov, F. Bociort, and J.J.M. Braat, "Birefringence induced by the spatial dispersion in deep UV lithography: theory and advanced compensation strategy", (to be published in *Optical Review*, 2005)
9. Code V 9.5 Reference Manual, (Optical Research Associates, August 2004).
10. R. Bunau, C. Hebbnd-Sollner, H. Holderer U.S. Patent US6784977 (2004).
11. N. Shiraishi, U.S. Patent US6775063(2004).
12. N. Shiraishi, Y. Omura, U.S. Patent Application US2003/0011893A1(2003).
13. M. Gerhard, D. Krähmer, German Patent DE 10133841A1 (2003).
14. J. Hoffman, J. McGuire, U.S. Patent US6683710 (2004).
15. T. Takahashi, J. Nishikawa, Y. Omura, U.S. Patent US6757051 (Embodiment 1).
16. D. Allan, J. Webb, J. Bruning U.S. Patent US6785051(2004).
17. K. Doyle, J. Hoffman, V. Genberg, and G. Michels, "Stress birefringence modeling for lens design and photonics", *Proc. SPIE Int. Soc. Opt. Eng.* 4832, 436-447 (2002).
18. J. Webb, J. Bruning U.S. Patent Application US2003/0168597A1(2003).